Structural Characterization of LDPE/EVA Blends Containing Nanoclay-Flame Retardant Combinations

Eduardo Ramírez-Vargas,[1] Saúl Sánchez-Valdes,[1] Octavio Parra-Tabla,[2] Sergio Castañeda-Gutiérrez,[2] Juan Méndez-Nonell,[1] Luis Francisco Ramos-deValle,[1] Adriana López-León,[1] Roberto Lujan-Acosta[1]

[1]*Centro de Investigación en Química Aplicada, Blvd Enrique Reyna 140, CP 25253 Saltillo, Coahuila, México*
[2]*Centro de Investigación y Desarrollo CONDUMEX, Carr. Constitución Km. 9.6, Parque Jurica, CP 76120, Querétaro, México*

Received 28 October 2010; accepted 25 March 2011
DOI 10.1002/app.34586
Published online 9 August 2011 in Wiley Online Library (wileyonlinelibrary.com).

ABSTRACT: The combination of different types of organo-modified montmorillonite (MMT) with aluminum hydroxide (aluminum trihydrate—ATH), as a flame retardant system for polyethylene-ethylene vinyl acetate (LDPE/EVA), blends were studied. Five different types of organically modified montmorillonite clays, each with different modifier, were used. The structural characterization was carried out by X-ray diffraction (XRD) and scanning electron microscopy in transmission mode (STEM). The mechanical and rheological properties were also evaluated. The XRD analysis showed a clear displacement of the d_{001} signal, which indicates a good degree of intercalation, especially for the MMT-I28 and MMT-20, from Nanocor and Southern Clay Products, respectively. The presence of ATH and the compatibilizer did not have any effect on the exfoliation of the studied samples. The thermal stability and flame retardant properties were evaluated by thermogravimetric analysis (TGA), limiting oxygen index (LOI—ASTM D2863), and flammability tests (Underwriters Laboratory—UL-94). The effect of different compatibilizers on the clay dispersion and exfoliation was studied. The results indicated that the addition of montmorillonite makes it possible to substitute part of the ATH filler content while maintaining the flame retardant requirements. The thermal stability of MMT/ATH-filled LDPE/EVA blends presented a slight increase over the reference ATH-filled LDPE/EVA blend. Compositions with higher clay content (10 wt %) showed better physicochemical properties. The increased stability of the higher clay content compositions results from the greater inorganic residual formation; this material has been reported to impart better performance in flammability tests. The mechanical properties and flame retardancy remained similar to those of the reference compound. The reduced ATH content resulted in lower viscosities and densities, facilitating the processing of the polymer/ATH/clay compounds. Extrusion of these compounds produced a lower pressure in the extrusion head and required reduced electrical power consumption. © 2011 Wiley Periodicals, Inc. J Appl Polym Sci 123: 1125–1136, 2012

Key words: nanocomposites; montmorillonite; aluminum hydroxide; LDPE/EVA blends

INTRODUCTION

Low-density polyethylene (LDPE) and polyethylene-*co*-vinyl acetate (EVA) exhibit an attractive combination of low cost, low density, and versatility in terms of properties, applications, and recycling. Polyethylene (PE), EVA, and their blends have been widely used in the cable industry, which in addition to stiff mechanical requirements, demands high flame-retardant performance. Because of their highly aliphatic hydrocarbon structure, LDPE and EVA are very flammable. These materials burn very rapidly, with a relatively smoke-free flame, and without leaving any char residue behind. The addition of flame retardants is thus needed to achieve the fire resistant properties required by the standards. Although the introduction of conventional flame retardants into these polymers is possible, high concentrations are required to comply with the standards. This negatively affects the processability and mechanical properties of the resulting compositions.

The use of halogen-free flame retardants is widespread, due to the concern about health and environmental risks.[1-4] Halogen-free flame retardancy is commonly achieved by the incorporation of inorganic fillers—typically aluminum trihydrate (ATH) or magnesium hydroxide [$Mg(OH)_2$]—into the polymer matrix. Although these fillers are essentially non-toxic and relatively inexpensive, the high levels required for adequate flame retardancy often lead to processing difficulties and marked deterioration in other critical polymer characteristics (e.g.,

Correspondence to: E. Ramírez-Vargas; saul@ciqa.mx or S. Sánchez-Valdes; evargas@ciqa.mx.
Contract grant sponsor: CONACyT; contract grant numbers: CB-24606/49143, CB-84424, CB-104865.

© 2011 Wiley Periodicals, Inc.

TABLE I
Sample Codes and Main Characteristics

Code	Organic modifier	Modifier conc. (wt %)*	d_{001} (nm)**
MMT-20[a]	*N*-Di-methyl dihydro-di-tallow amonia chloride	38.7	2.43
MMT-I28[b]	*N*-Octadecyl trimetyl amine chloride	32.9	2.42
MMT-15[a]	*N*-Di-methyl dihydro-di-talow ammonia chloride	43.2	3.18
MMT-30[a]	*N*-Methyl, talow.bis-2-hydroxietyl, ammonia chloride	30.1	1.82
MMT-NFS[a]	Dimethyl, di(hydrogenated tallow) alkyl ammonium chloride	28.3	3.25

[a] Southern Clay Products Inc.
[b] Nanocor Inc.
* Measured by TGA analysis.
** Measured by XRD.

mechanical, physical, and electrical properties). The addition of compatibilizers can improve the compatibility of fillers to matrix polymers. This has a great effect on the mechanical properties of the composites.[5,6]

Because of their improved fire resistant properties, nanocomposites formed from a polymer matrix and layered silicates have attracted considerable interest from investigators studying flame retardant polymer compositions.[7-9] It has been demonstrated that the presence of clay in a polymer matrix can enhance the char formation. This provides a transient protective barrier, slowing the matrix burning process.[9,10] Using the cone calorimeter, the flammability properties of a variety of polymer–clay nanocomposites[11,12] has revealed improved flammability properties in terms of reduced peak heat release rates. However, the values from the limiting oxygen index and other flame retardant tests show no significant improvement when the nanoclays are added.[13,14] Therefore, the use of layered silicates as the single flame retardant filler is limited; however, the combination with other flame retardants is highly interesting, due to the possibility of synergism.[15] Synergistic combinations allow for a higher effectiveness of the flame retardant system. This in turn allows for reductions of flame retardant loading, with fewer drawbacks. Some reported synergistic systems include combinations of aluminum or magnesium hydroxides with layered silicates[16-19] and other additives.[20-22] Other authors[23] have reported the substitution of a certain fraction of phosphorous flame retardant by nanoclay obtaining improved flame retardant properties. More recently, some polymer nanocomposites have been successfully commercialized[24,25] as having improved flame retardant properties.

To improve the thermal stability of polyethylene, it is cross-linked in the presence of either peroxides or silanes. The polyethylene crosslinking improves the thermal stability, fire retardancy, and mechanical properties of the metallic hydroxide filled polyethylene.[26,27]

Different montmorillonite (MMT) and aluminum hydroxide (ATH) combinations are studied on a LDPE/EVA blend to investigate their effect on the flame retardancy and the mechanical and rheological properties. The goal of this work was to develop a PE/EVA compound using nanoclays and reduced ATH content. The idea is to design such a compound with flame retardant characteristics similar to those of a referenced polyolefin compound, while also offering lower density and better rheological and processing characteristics.

EXPERIMENTAL

Materials

The LDPE was from Dow Plastics with a melt index of 2.5 g/10 min. Polyethylene-*co*-vinyl acetate (EVA) from DuPont with 28% vinyl acetate and a melt index of 3.0 g/10 min was used. The ATH was supplied by Aurum Chemical. The compatibilizers used were a maleated LLDPE Bynel 4107 (PEgMA) and a maleated EVA Bynel 3095 (EVAgMA) both from DuPont, with 0.9 and 0.6 wt % maleic anhydride groups and a melt index of 0.91 and 2.3 g/10 min, respectively. A Zn neutralized ionomer, Surlyn 1652, from DuPont, with 6.5 wt % methacrylic acid and a melt index of 5.2 g/10 min was also used. The nanoclays used, along with their characteristics, are given in Table I.

Samples preparation

The polymeric matrix used was a blend of LDPE and EVA in a 70/30 ratio. The filled composites were prepared using a Werner and Pfleiderer corrotating twin screw extruder with an $L/D = 29{:}1$ and $D = 30$ mm, operating at 190°C and 100 rpm. Samples in this study were not crosslinked. Thereafter, the compounds were compression molded at 185°C to obtain 150 mm × 150 mm × 2 mm plates from which test specimens were cut. The total ATH filler loading was reduced from 53 to 47, 43, and 38 wt %, and was substituted by 6 or 10 wt % of MMT.

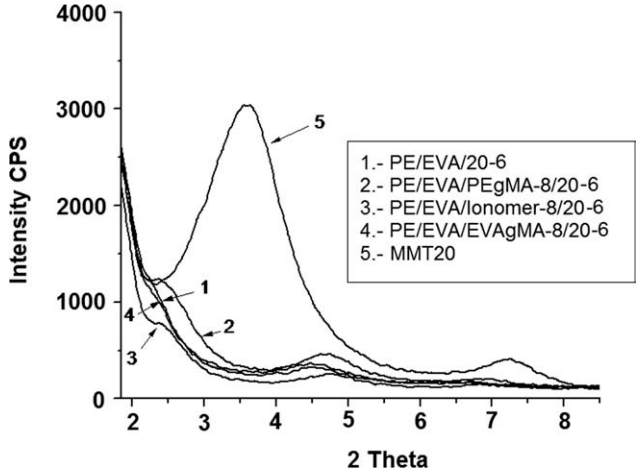

Figure 1 XRD patterns of MMT-20 clay, LDPE/EVA with 6 wt % clay, and PE/EVA with 6 wt % clay plus 8 wt % of the three different compatibilizers.

Characterization

To evaluate the evolution of the clay d_{001} reflection, X-ray diffraction of the modified clays and nanocomposites, was performed in a Siemens D5000 using CuKα X-ray radiation. To minimize a preferred orientation of the clay, the samples for X-ray analysis were obtained from the compression molded plates. Ultrathin sections for STEM analysis, 70–100 nm thick, were cut from the compression molded plates with a diamond knife using a Leica microtome.

The STEM observations were performed using a Jeol-JSM-7401F FESEM, with a STEM modulus and a field emission gun at an accelerating voltage of 200 kV. Fractured surfaces for SEM analysis were obtained from the compression molded plates; they were fractured at liquid nitrogen temperature and then coated with an Au/Pd alloy. The SEM observations were carried out using a Top Con 510 SM. Tensile properties were analyzed on an Instron tensile testing machine, model 4301, at an extension rate of 5 mm/min, in accordance with ASTM D-638. Thermogravimetric analyses (TGA) were carried out with a TA Instruments TGA-Q500 analyzer, at a heating rate of 10°C/min under nitrogen flow.

Two standard test methods were used to evaluate the fire-retardant properties of nanocomposite systems: (a) the limiting oxygen index (LOI) test, which was carried out on 120 mm $\times$ 7 mm $\times$ 5 mm specimens, in accordance with BS 2782, using a Fire Testing Technologies Ltd instrument; and (b) the UL-94 vertical burning test, which was carried out on 120 mm $\times$ 7 mm $\times$ 5 mm specimens, according to UL-94. The rheological behavior was measured with a capillary rheometer (Instron 4467), using a die with an L/D of 27.55 and $D = 1$ mm, at 195°C. All tests were done in triplicate. Density measurements were obtained by picnometer technique according to ASTM D297.

RESULTS AND DISCUSSION

Selection of compatibilizer and nanoclay

XRD characterization

The effect of a compatibilizer on the clay dispersion and exfoliation was analyzed by XRD. The compatibilizers were PEgMA, EVAgMA, and an ethylene—methacrylic acid ionomer. Figure 1 shows the effect of the three different compatibilizers on the XRD patterns of the corresponding PE/EVA nanocomposites, with 6 wt % clay and 8 wt % of compatibilizer. The original basal reflection peak of MMT-20 appears at 3.6°, which corresponds to an intergallery spacing of 2.43 nm. The peaks of the PE/EVA/clay nanocomposites with and without compatibilizer, on the other hand, shift to lower angles. The reflection peaks of composites with PEgMA and ionomer appear near 2.4° (3.6 nm), whereas the reflection peaks of the sample with and without EVAgMA compatibilizer disappear. This suggests an intercalated structure for the ionomer and PEgMA samples and an exfoliated morphology for nanocomposites with and without EVAgMA as compatibilizer. This also suggests that the use of a compatibilizer has quite a small impact on the clay exfoliation. This could be explained by the more favorable interaction between vinyl acetate (VA) groups from EVA and nanoclay, which have been described previously,[28] than the MA and Ionomer groups.

To determine the most adequate type of nanoclay for this study, nanocomposites were analyzed by XRD to measure the intergallery spacing. Figure 2 shows the XRD results for the five organomodified clays with their corresponding peak intensities and peak angles. These relate to the intergallery spacing

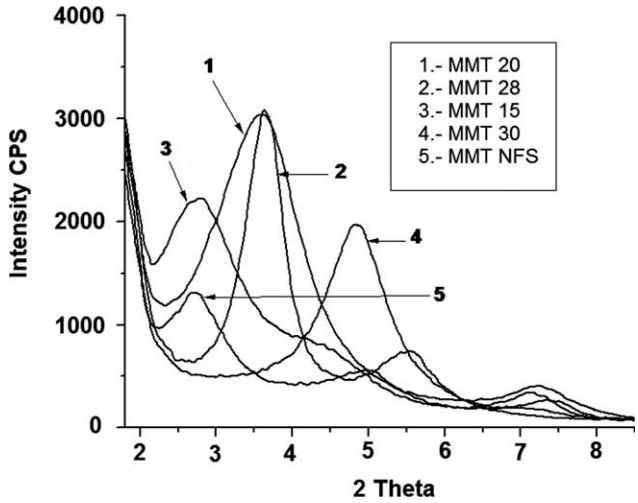

Figure 2 XRD patterns of the five different clays studied.

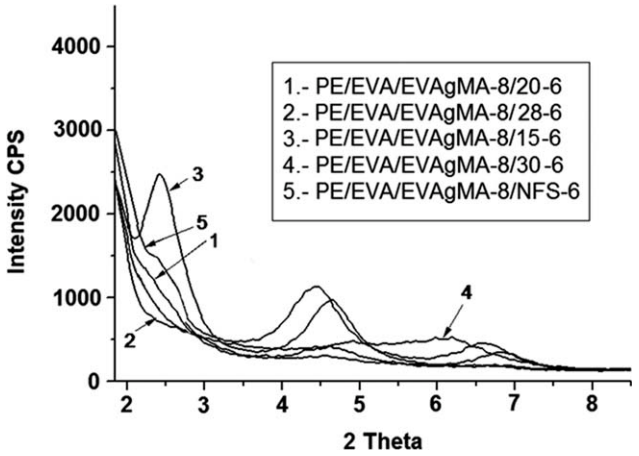

Figure 3 XRD patterns of LDPE/EVA nanocomposites with 8 wt % of EVAgMA compatibilizer and 6 wt % of each of the five different clays studied.

and eventually, to the degree of exfoliation in the nanocomposite. This figure, as well as Table I, show that MMT-20 and I28 have a similar intergallery spacing of 2.43 nm and 2.42 nm, respectively. However, MMT-20 has a broader signal indicating that a more disordered intercalated structure might be obtained with this rather than with MMT-I28. On the other hand, MMT-15 and MMT-NFS both have a greater intergallery spacing, that is, 3.18 nm and 3.25 nm, respectively, and similar peak broadness. MMT-30 has the lowest intergallery spacing (1.18 nm) of all the considered clays.

It has been reported that the intensity and sharpness of the reflection peak depend on the intercalated/exfoliated structure. A more intense and sharp peak are indicative of a more ordered intercalated structure, whereas a less intense and broader peak are indicative of a disordered intercalated structure, that is closer to an exfoliated one.[29]

Figure 3 shows the XRD results for the PE/EVA nanocomposites with 6 wt % of each of the five different clays and 8 wt % of EVAgMA as compatibilizer. In the nanocomposite with MMT-15 clay, the original peak of the clay (2.77°, 3.18 nm) shifts to only 2.4°, corresponding to an intergallery spacing of 3.66 nm. For the MMT-30 clay, the reflection peak d_{001} was displaced to higher diffracting angles, from 4.8 to 6.0° (1.82–1.46 nm). This indicates an overall decrease in the layer periodicity. This indicates that these clays induce a poor intercalation to these composites. These results have been reported by other authors[28] and were attributed to the higher modifier concentration for MMT-15 (43 wt %) from Table I. This implies a higher degree of substitution of the original exchangeable cations, which limits the free ingress of the polymer chains through the clay galleries due to steric hindrance. Additionally, for MMT-30, this behavior was attributed by some authors[30] to the thermal degradation of the surfactant. Other authors[28] suggests that even though this clay has a surfactant with more polar groups, the degree of saturation of the exchangeable cations and the lower initial intergallery spacing (1.82 nm) are the main factors affecting this nanoclay exfoliation. The main basal reflection d_{001} peak of pure MMT-NFS is observed at 2.7° (3.2 nm). Meanwhile, in the nanocomposite, the reflection peak appears at 2.3° (3.7 nm), a shift of only 0.4°. This indicates a similar structure than MMT-30 and MMT-15 clays. On the other hand, clays MMT-20 and MMT-I28 show the more noticeable shift of the reflection peak to lower angles. The composite containing clay MMT-20 shows a noticeable shift from 3.6° (2.43 nm) to 2.2° (3.9 nm). Meanwhile, for the sample with clay MMT-I28, this peak has even disappeared. This indicates a much better dispersed and exfoliated structure for these composites.

Since the x-ray diffraction patterns are an average of the repetitive crystallographic planes of the nanoclay, it is possible to identify an intercalated layer structure by this technique. However, TEM is necessary to clearly identify an exfoliated structure.

STEM characterization

Figure 4 presents the STEM micrographs of the composites with 6 wt % clay, MMT-20 (a and b), MMT-I28 (c and d), and MMT-NFS (e and f). (a, c, and d), on the left, without compatibilizer and (b, d, and f) on the right, with 8 wt % of EVAgMA. It can be observed that, with all three clay types, the effect of using a compatibilizer is negligible. For MMT-20, MMT-I28, and MMT-NFS clay samples, the morphologies with and without compatibilizer are quite similar. Only a few clay aggregates can be observed, especially for the MMT-NFS sample; however, most of them are well exfoliated which is in agreement with the corresponding XRD results. The samples with MMT-20 and I28 showed a greater degree of exfoliation than the NFS samples which is in agreement with the XRD results. Thus, according to the results presented above, it was decided to use the MMT-20, MMT-I28, and MMT-NFS clays without compatibilizer to incorporate the flame retardant and continue with the study.

Nanoclay-flame retardant combinations

XRD characterization

Figures 5–7 show the XRD results of LDPE/EVA composites with 6 and 10 wt % of each of the three clays studied, all with 43 wt % of ATH. Vaia and Giannelis[29] proposed that an increase in the intergallery spacing would result in a new diffraction pattern, which would correspond to the increased spacing of the clay galleries. According to these

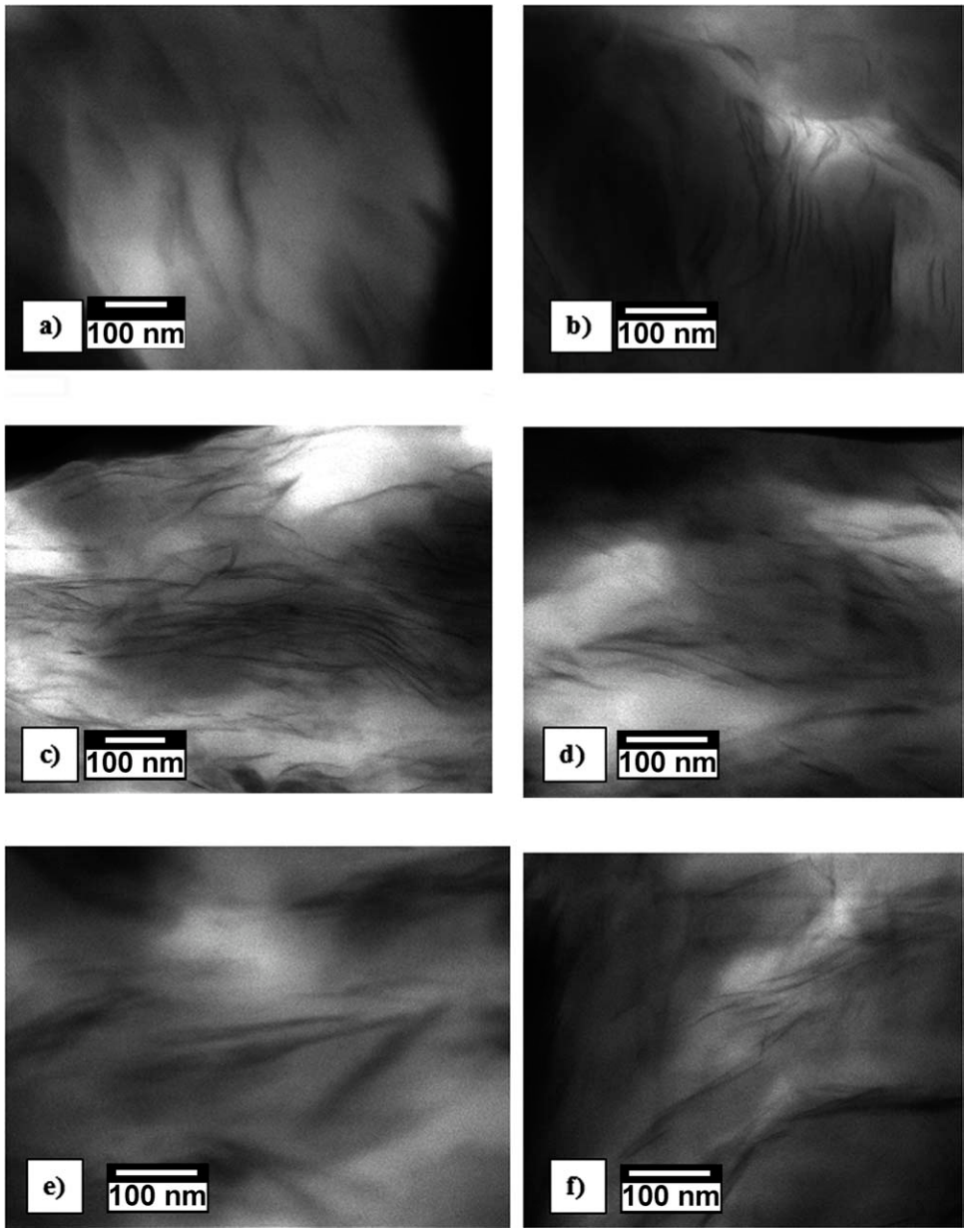

Figure 4 STEM micrographs of LDPE/EVA nanocomposites without compatibilizer and 6 wt % of MMT: (a) 20, (c) I28, (e) NFS and with 8 wt % of EVAgMA compatibilizer and 6 wt % of MMT: (b) 20, (d) I28, (f) NFS.

authors, the degree of intercalation/exfoliation in the composite could be determined by changes in the intensity and sharpness of the corresponding reflection peaks.

In the samples with 6 wt % of MMT-20 clay, the peak characteristic of the d_{001} of MMT-20 (3.6°) is displaced to lower angles for all nanocomposite materials (Fig. 5). The composites showed peaks with less intensity and broader less defined signal, indicating that a more disordered intercalated layer structures might be obtained. This figure shows that, for MMT-20 at 6 wt % the diffraction peak has disappeared. This suggests that an exfoliate structure has been obtained with a resulting increase in the average intergallery spacing. For this clay content, the ATH content has no significant effect on the clay dispersion. Meanwhile, the samples with 10 wt % of MMT-20 show quite similar shifts to lower angles. However, the diffraction peak has a higher intensity with a more defined signal and less broadening. This indicates a more ordered layer structure, which has been attributed by other authors[31] to clay saturation when using higher clay loadings. The van der Waals attraction force between clay layers becomes dominant as the distance that separates these layers becomes smaller.[31,32] At higher ATH contents, on the other hand, the viscosity increases. The higher shear during melt mixing, due to the higher

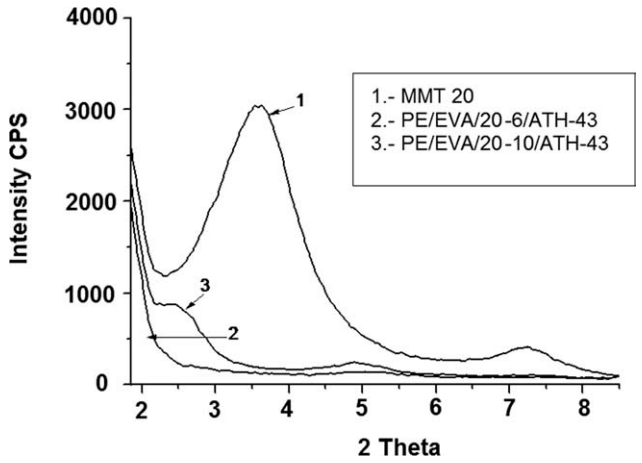

Figure 5 XRD patterns of MMT-20 clay and of LDPE/EVA nanocomposites with 43 wt % of ATH and 6 and 10 wt % of 20 clay.

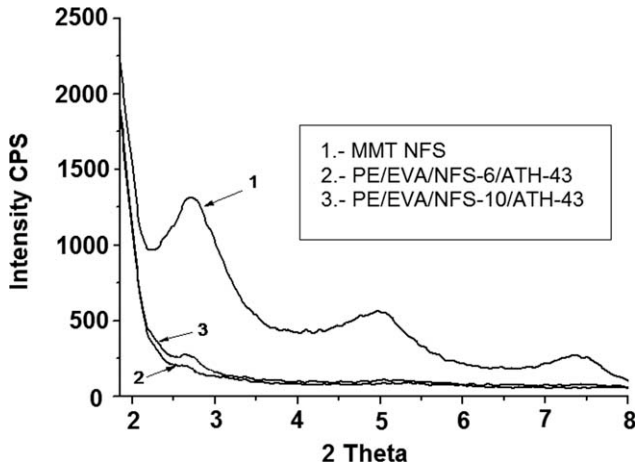

Figure 7 XRD patterns of MMT-NFS clay and of LDPE/EVA nanocomposites with 43 wt % of ATH and 6 and 10 wt % of NFS clay.

viscosity, results in a better clay exfoliation. This has been corroborated via XRD with a shift to lower diffraction angles.

Even MMT-15 and MMT-20 have the same surfactant structure (Table I), MMT-20 has lower modifier concentration which leaves more room for the free ingress of the polymer chains through the clay galleries, which eventually results in an intercalated or exfoliated structure.

When using MMT-I28 clay at 6 and 10 wt % (Fig. 6) no diffraction peak was observed. This may indicate the possibility of having higher exfoliated or intercalated silicate nanolayers of clay dispersed in the polymer matrix. This could be attributed to a strong interaction between the vinyl acetate groups of EVA and this nanoclay polar surfactant, which would lower its surface energy and enhance its dispersion on the polymer matrix. When using 10 wt % of this clay, no signal of clay saturation was observed.

The comparison of the spectrum with that of the neat MMT-NFS (Fig. 7) shows that there is a shift from 2.7° 2θ. This corresponds to an intergallery spacing of 3.2 nm, for the neat clay, compared with 3.5 and 3.6 nm for the nanocomposite samples at 6 and 10 wt %, respectively. This slight shift suggests that the intercalation with this clay was less significant than with the other two clays. This indicates that the chemical structure of the surfactant of this clay has less favorable interactions that could enhance its exfoliation in the polymer matrix.

This indicates the possibility of obtaining a more dispersed and exfoliated structure in the samples with MMT-I28 and MMT-20 than with MMT-NFS. However, these assumptions need to be confirmed by STEM analysis.

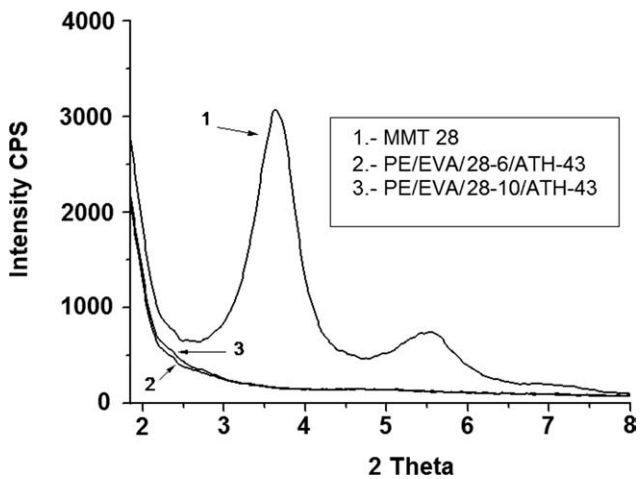

Figure 6 XRD patterns of MMT-I28 clay and of LDPE/EVA nanocomposites with 43 wt % of ATH and 6 and 10 wt % of MMT-I28 clay.

STEM characterization

Figures 8 and 9 show the STEM images (carefully selected from at least 20 images from different parts of the sample) of LDPE/EVA with 10 wt % of MMT-20, MMT-I28, and MMT-NFS clays with 38 wt % (Fig. 8) and 43 wt % (Fig. 9) of ATH. At these magnifications, ATH flame retardant particles and exfoliated clay platelets can be observed. A better exfoliation can be observed on samples with 43 wt % of ATH, as compared with 38 wt %. This is in agreement with the XRD results, where the diffraction peak shifted to lower 2θ angles when using higher ATH contents. This suggests that the dispersion state is increased by the addition of a fire retardant. It appears that the presence of ATH helps in the exfoliation-dispersion of the clay. Similar results have been reported by other authors[33] in a PP/Clay/Fire-Retardant combination. This could be

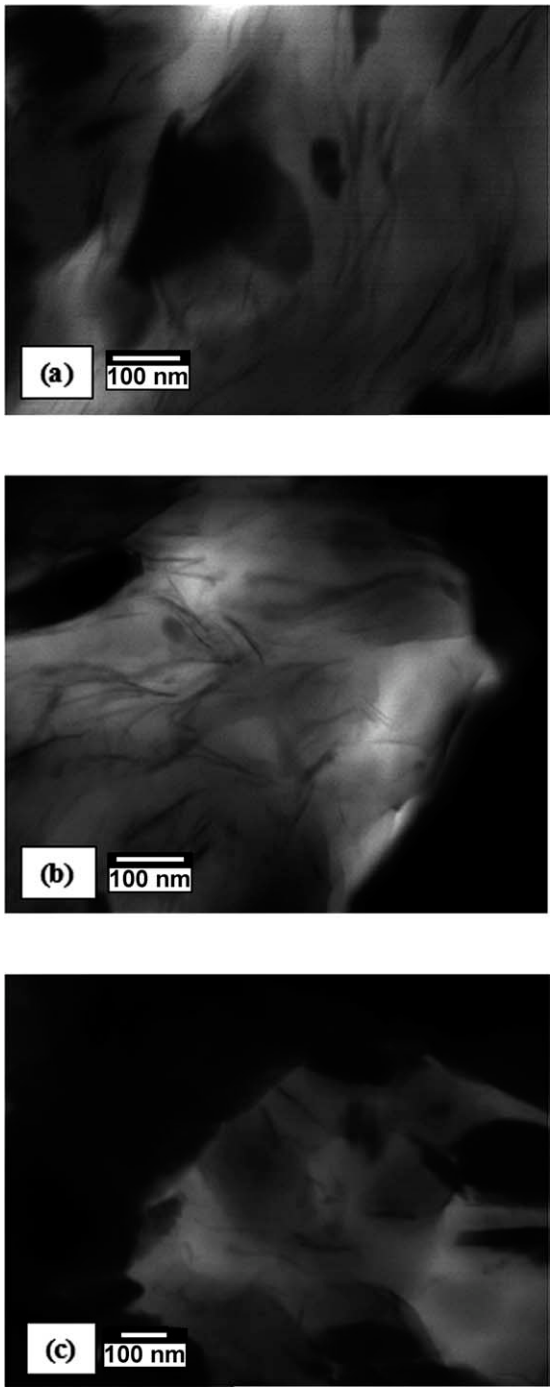

Figure 8 STEM micrographs of LDPE/EVA nanocomposites with 38 wt % of ATH and 10 wt % of MMT: (a) 20, (b) I28, and (c) NFS clays.

attributed to an increased melt viscosity with higher ATH contents that in turn could increase the shear stress that favors the clay exfoliation-dispersion. However, further investigation is needed to clarify these observations.

Clay exfoliation is clearly evident in these micrographs for samples with 10 wt % of MMT-20 and MMT-I28, where a more uniform distribution with less tactoids can be seen. Individual clay layers can be observed. These are indicative of a greater degree of exfoliation of the MMT-I28 clay, as suggested by the XRD results (Fig. 6). No peak was generated by these composites. Images of the MMT-NFS clay composites, on the other hand, show many clay aggregates or tactoids. These results are also consistent with those from XRD (Fig. 7), where this clay showed the less noticeable shift to lower 2θ angles.

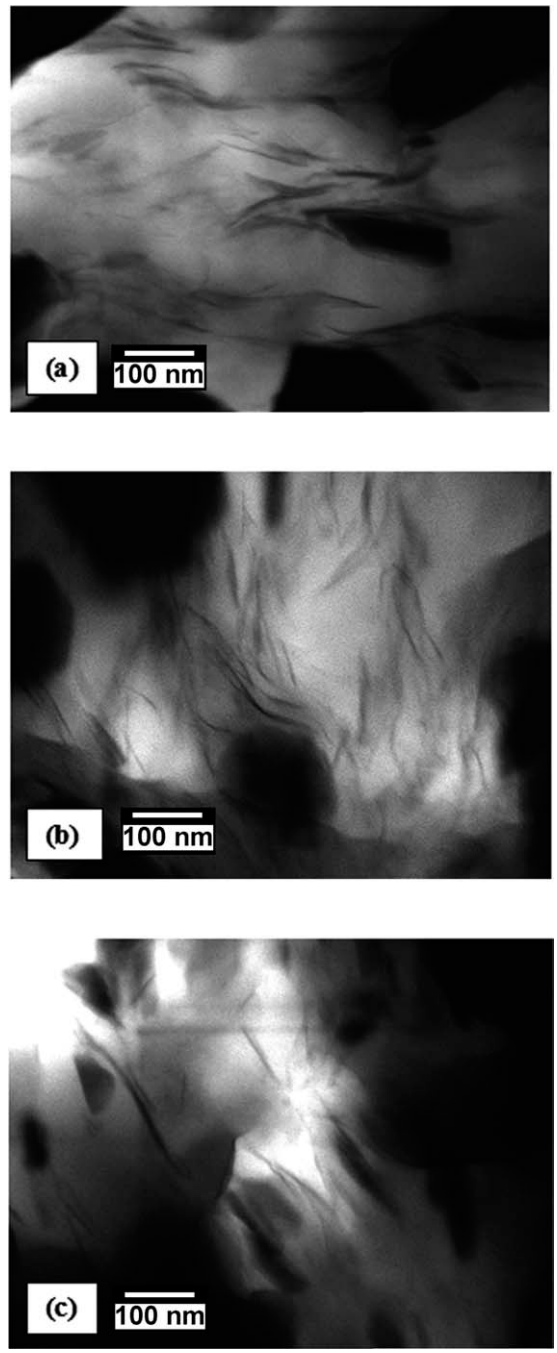

Figure 9 STEM micrographs of LDPE/EVA nanocomposites with 43 wt % of ATH and 10 wt % of MMT: (a) 20, (b) I28, and (c) NFS clays.

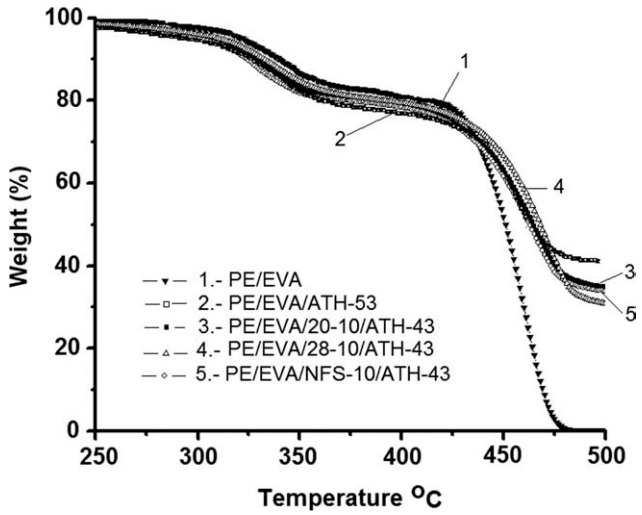

Figure 10 TGA curves of pure LDPE/EVA and of LDPE/EVA nanocomposites with 43 wt % of ATH plus 10 wt % of MMT-20, I28, and NFS clays.

Thermal stability

The thermal behavior of ATH has been discussed in several works.[34] Between 190 and 350°C, ATH will decompose endothermically in a single step, with a mass loss of 35%. The thermal degradation of LDPE/EVA takes place in two steps which tend to overlap in oxidative conditions. The first one, occurring between 300 and 380°C, corresponds to the deacylation of the vinyl acetate groups in EVA. The second step meanwhile, occurs around 390–480°C, and is attributed to the degradation of the hydrocarbon chains.[35] The LDPE/EVA blend used had a composition ratio of 70/30 and shows a deacylation stage at 315°C (see Fig. 10).

After the EVA deacylation stage (i.e., from 410 to 475°C), the filled LDPE/EVA blends (10 wt % clay and 43 wt % ATH) present a marked decrease in the degradation rate when compared to the unfilled blend. As can be observed in this figure, in the first step, the decomposition of the ATH filled sample started at lower temperature. This behavior is assigned to the ATH endothermic decomposition, which takes place between 190 and 350°C. Comparing the nanocomposite samples, only small differences between them can be observed. Nanocomposites with MMT-NFS showed a slightly higher weight loss and the samples with MMT-I28 showed the lowest weight loss. This can be attributed to the better dispersion grade obtained with this clay.

In the second step, at higher decomposition temperatures (between 400 and 470°C), a greater decomposition rate for the neat polymers can be observed. Meanwhile, the filled nanocomposites showed a lower decomposition rate. The reference sample, with only ATH as filler, shows lower thermal stability in this second step.

Comparing the effect of the different nanoclays, the MMT-I28 clay shows a slightly higher temperature for the onset of the degradation of the hydrocarbon chains (441°C) than the MMT-20 and NFS clays (around 430°C). This effect has been related to the differences in the dispersion and exfoliation morphologies. The higher the degree of exfoliation the better the mass transport barrier for the volatile products generated during decomposition.

Comparing the flame retardant systems combinations, it can be concluded that the presence of MMT in the flame retardant systems enhanced the thermal stability of the polymer blend matrix. This behavior has been reported to occur as a consequence of the gas barrier effect exerted by the MMT when dispersed in the polymer matrix.[36]

The inorganic residue at 600°C determined by TGA analysis showed a content of 40 wt % for the reference sample containing 53 wt % of ATH. This residue was 42 wt % for the sample containing 6 wt % clay and 47 wt % ATH and 44 wt % for the sample containing 10 wt % clay and 47 wt % ATH. This indicates that the inclusion of even small amounts of clay promotes the formation of more inorganic residue, which in turn is responsible for the slightly increased stability observed with the higher clay content compositions. Similar results have been reported by Beyer[4] who found that when exposed to flame, the formation of an intumescent layer is the main responsible for the improved flame retardancy of an EVA/ATH/Clay nanocomposite. Other authors[37,38] have reported that clay nanocomposites show considerable effect in promoting the formation of an intumescent layer, and provide a greater reduction in the cone calorimeter heat release rate, as compared with that obtained with microcomposites.

Flammability test results

Table II lists the LOI and UL-94 data obtained for the LDPE/EVA compositions studied. Although the LOI test (which establishes the minimum concentration of O_2, as the percentage of a nitrogen/oxygen mixture, that will support combustion of a polymer sample) is widely used and generally considered reproducible for a given sample, it is important to note that results from the LOI method often have little correlation with flammability performance in other laboratory test procedures (particularly with the widely reported UL94 vertical burn ignition test). In this test, the samples are exposed to a burner flame for 10 s. The flame is then retired, and the time it takes for the flame to extinguish is designated as t_1. Immediately thereafter, the procedure is repeated, and the time is now designated as t_2. Finally, the time the sample remains glowing or

TABLE II
Combustion Parameters Obtained from LOI and UL-94

Sample	LOI	UL-94 (time to extinguish, s) t_1	t_2	t_3
LDPE/EVA	19.0	*	*	*
LDPE/EVA/ATH-53 (Reference)	27.0	53	95	53
LDPE/EVA/MMT28-6/ATH-47	27.5	36	76	19
LDPE/EVA/MMT28-10/ATH-47	27.7	22	53	15
LDPE/EVA/MMT28-10/ATH-43	26.0	52	78	90
LDPE/EVA/MMT28-10/ATH-38	25.5	70	100	135
LDPE/EVA/MMT20-10/ATH-47	27.5	24	98	123
LDPE/EVA/MMT20-10/ATH-43	24.5	60	101	143
LDPE/EVA/MMT20-10/ATH-38	24.5	90	128	*
LDPE/EVA/MMTNFS-10/ATH-47	24.0	71	89	*
LDPE/EVA/MMTNFS-10/ATH-43	23.5	82	99	*
LDPE/EVA/MMTNFS-10/ATH-38	23.0	90	102	*

* Samples were burnt completely.

incandescent (after t_2) is taken as t_3. To be rated by UL94 either as V-0, V-1, or V-2, ($t_2 + t_3$) must be $<$60 s. But, as observed in Table II, all samples failed to comply with this test.

Nonetheless, the results presented in Table II give information about the flammability performance of the different samples. Pure LDPE/EVA shows an LOI value of 19 (very low), and burns completely in the UL94 test. Samples with ATH and MMT clays, on the other hand, show higher LOI values. The reference sample, with 53 wt % ATH, shows an LOI of 27 and low after-flame times. This is due to the very high ATH content. However, the LOI values increased when substituting a percentage of ATH with montmorillonite. For instance, higher clay loadings (10%) in combination with ATH (47%), especially MMT-I28, resulted in higher LOI values (27.7) and relatively lower extinguishing times. The LOI values increased in a negligible amount from 27.5 to 27.7 when the MMT-I28 clay content increased from 6 to 10 wt %. Lower LOI values and high after-flame times were obtained for the lower ATH content (38 wt %). Considering the combinations with clay, the lowest LOI values (23) and the worst behavior in the UL94 test were obtained when using MMT-NFS clays. This was attributed to the lower degree of dispersion and exfoliation obtained with this clay.

It is inferred that the better ATH dispersion and better MMT-20 and I28 clay exfoliation are responsible for the increase in LOI. This can be explained as follows, in the combustion of these nanocomposites the better dispersed flame retardant particles would be heated homogeneously and its water release would be accelerated as well as the better exfoliated clays would enhance the barrier to the volatile products generated during decomposition.

These results are in agreement with those found in TGA analysis in which the composites with MMT-I28 showed slightly higher decomposition temperature indicating a better thermal stability.

The different behavior observed for these nanoclays (MMT-20, I28, and NFS) could be related with the differences in their organic modifier structures. MMT-20 and MMT-NFS both have a similar modifier structure with two hydrocarbon chains, whereas MMT-I28 has only one hydrocarbon chain (Table I). This difference in hydro carbonated tallow chains could be the reason why MMT-I28 presented in general better behavior, since its organic modifier, with only one tallow chain, would offer less steric hindrance for the penetration of the polymer chains and hence allowing better intercalation and exfoliation than the other clays.

With respect to the dripping characteristics of the samples, we found that none of the clay-ATH nanocomposites showed any dripping at all, even those in which 10 wt % of ATH was substituted by the equivalent wt % of clay. The only sample that showed a significant dripping was the LDPE/EVA compound without any filler.

Physical–mechanical properties

It is known that a homogeneous dispersion of clay nanolayers in a polymer matrix would provide maximum reinforcement. Interactions between exfoliated nanolayers with a large interfacial area and the surrounding polymer matrix would lead to higher tensile strength, modulus, and thermal stability. Conventional polymer–filler composites containing micron-size tactoids also would improve stiffness and modulus, but at the expense of tensile strength, elongation, and toughness.

Table III presents the tensile properties of neat LDPE/EVA and the nanocomposites with the different clays and ATH. As expected, unfilled LDPE/EVA gave the highest elongation and the lowest hardness and tensile strength. As discussed before, a high content of ATH in polymers can adversely affect some mechanical properties; it often decreases their tensile strength.[39] An increase in the clay content (e.g., MMT-I28 from 6 to 10 wt %), has no effect on tensile strength, but increases the hardness and reduces the elongation at break. The higher ATH contents of 43 and 47 wt % with 10 wt % of clay, especially for MMT-I28 and 20 clays, show higher tensile strength and elongation at break and almost the same hardness than the reference sample with 53 wt % of ATH. Samples with lower ATH content (38 wt %) showed the higher elongation at break and a lower hardness. These improvements can be attributed to the lower total filler content and to the reinforcement effect of the nanoclay platelets. In comparing the effect of the different clay types, it can be seen that the composites with MMT-I28 and

TABLE III
Mechanical Properties and Density Measurements of PE/EVA Composites

Sample	Hardness (Shore-D)	T.S. (MPa)	Elongation at break (%)	Density (g/cm^3)
LDPE/EVA	40 ± 0.5	16.5 ± 1.0	595 ± 15	0.931 ± 0.01
LDPE/EVA/ATH-53 (Reference)	51 ± 0.8	13.0 ± 0.2	170 ± 9	1.42 ± 0.03
LDPE/EVA/MMT28-6/ATH-47	50 ± 1.8	16.1 ± 0.6	251 ± 21	1.38 ± 0.05
LDPE/EVA/ MMT28-10/ATH-47	51 ± 1.0	15.9 ± 0.3	198 ± 31	1.40 ± 0.04
LDPE/EVA/ MMT28-10/ATH-43	49 ± 0.5	15.5 ± 1.5	305± 23	1.31 ± 0.06
LDPE/EVA/ MMT28-10/ATH-38	48 ± 0.9	13.9 ± 0.2	326 ± 37	1.29 ± 0.09
LDPE/EVA/ MMT20-10/ATH-47	52 ± 1.1	16.7 ± 0.3	202 ± 18	1.40 ± 0.07
LDPE/EVA/ MMT20-10/ATH-43	50 ± 0.7	15.7 ± 0.5	315 ± 11	1.34 ± 0.09
LDPE/EVA/ MMT20-10/ATH-38	47 ± 0.2	14.3 ± 0.4	336 ± 10	1.30 ± 0.03
LDPE/EVA/MMTNFS-10/ATH-47	50 ± 0.6	13.6 ± 0.5	361 ± 08	1.39 ± 0.02
LDPE/EVA/MMTNFS-10/ATH-43	49 ± 1.0	13.4 ± 0.9	446 ± 14	1.34 ± 0.10
LDPE/EVA/MMTNFS-10/ATH-38	46 ± 0.8	13.1 ± 1.2	465 ± 11	1.30 ± 0.07

20 showed a higher stiffness and ductility than the samples with NFS. This can be attributed to the higher degree of dispersion and exfoliation obtained with these clays. The results corroborate that substitution of part of ATH with nanoclay, to obtain an ATH/Clay nanocomposites, enhances both fire retardancy and mechanical properties.

This table also shows the density values obtained for the different samples. The reduction in the total ATH content by the inclusion of nanoclay originated a noticeable reduction in the density of the composites. As the ATH content is partly substituted by nanoclay, the density of the composites is reduced.

Rheological behavior

Understanding the rheological properties of these nanocomposites is not only important in gaining fundamental knowledge of the processability, but also in understanding the structure–property relationship in these materials. Figure 11 shows the shear rate dependence of the viscosity for the different nanocomposite samples. All the examined materials show a shear-thinning non-Newtonian behavior in the whole shear rate range. This behavior, typical of polymer melts, results from the disentanglement process and the increase of the average end to end distance of polymer chains that is caused by shearing. The viscosity of neat LDPE/EVA shows the lower values for the whole shear rates examined, whereas the reference with 53 wt % ATH shows the higher viscosity. A partial substitution of ATH with nanoclay shows a noticeable reduction in shear viscosity, especially at lower shear rates. This can be explained considering that at lower filler contents, the polymer chain flexibility is not significantly affected, which results in a reduction on the composite shear viscosity. Comparing the effect of the different clay types, especially at the lower shear rates MMT-I28 clay shows the higher viscosity followed by 20 and NFS. At higher shear rates, on the other hand, the effect of the different clays is negligible. This behavior is highly dependent on the degree of dispersion and exfoliation. The greater the level of polymer–clay interactions and the greater the level of clay dispersion and exfoliation, the greater the inhibiting effect on the chain flexibility. This results in an increase in the shear viscosity. Additionally, at high shear rates, the viscosities of the nanocomposites are almost the same, indicating a similar processability. This suggests that at high shear rates, the ATH and clay platelets become highly oriented toward the flow direction, which causes the shear viscosity of the nanocomposites to become nearly identical. This later effect may also be associated with the slippage of polymer chains over the nanoclay platelets.[40]

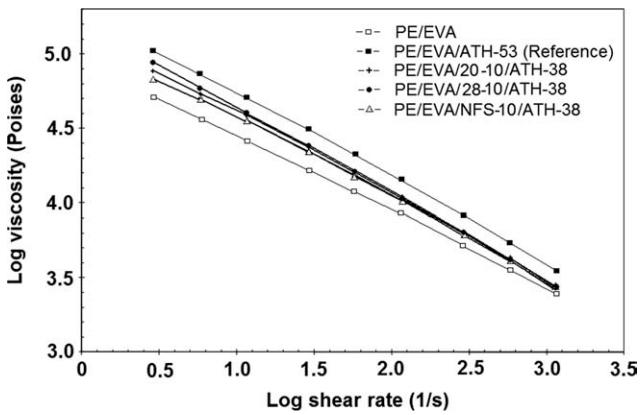

Figure 11 Shear viscosity versus shear rate for pure LDPE/EVA, the reference PE/EVA with 53 wt % ATH and the LDPE/EVA nanocomposites with 38 wt % ATH and 10 wt % of each of 20, I28, and NFS clays

Processability

MMT-I28 clay was selected as the most convenient clay for this study due to its exfoliation, mechanical,

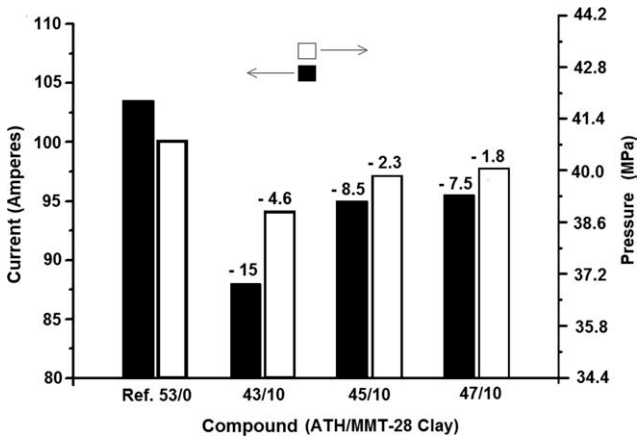

Figure 12 Decrease in current consumption and pressure at the extruder during extrusion processing of the fire retardant LDPE/EVA nanocomposites after partial substitution of ATH with each of the three better compound systems.

and fire resistance performance. Samples of LDPE/EVA with three ATH/Clay combinations (43/10, 45/10, and 47/10) were processed by an industrial processing system to characterize the real improvements in the processability of the formulated compounds. The extrusion of these compounds as cable jacketing required less pressure in the extrusion head, as well as less of a corresponding reduction in the amount of electrical power needed for the equipment. Figure 12 shows the processing improvements that occurred as a result of substituting part of the ATH with nanoclay, particularly MMT-I28.

CONCLUSIONS

The XRD analysis in this study showed a clear displacement for the d_{001} signal. This indicates a good degree of intercalation, especially with MMT-I28 and MMT-20 clays. The presence of compatibilizer did not have any significant effect on the exfoliation of these samples.

Compounds with higher clay content (10%) presented better flame retardancy than those with lower clay content. This was attributed to the fact that higher clay content results in a higher inorganic residual formation, which shows better performance in flame tests.

It can also be concluded that the properties of the obtained compounds with ATH and nanoclay are equivalent to those of the reference compound with ATH only. Formulations with MMT-I28 and MMT-20 clays presented a better degree of intercalation–exfoliation. The use of a compatibilizer did not show any superior behavior compared with those without.

A lower ATH content in the obtained compounds with clay, results in a lower density than that in the reference compound. It also exhibits better extrusion processability, which is beneficial for industrial production.

It can be concluded that the substitution of part of ATH by clay produces nanocomposites with similar flame retardant characteristics to the reference compound. Nevertheless, these obtained ATH-clay nanocomposites showed lower density, lower viscosity, and lower energy consumption during extrusion, which could represent economical advantages.

The authors thank Anabel Ochoa, Blanca Huerta, Miriam Lozano, Josefina Zamora, Marcelina Sánchez, Concepcion Gonzalez, Jesus Rodriguez, Fabian Chavez, Francisco Zendejo, Jose Lopez-Rivera, Patricia Siller, and Guadalupe Mendez for their technical support.

REFERENCES

1. Haurie, L.; Fernandez, A. I.; Velasco, J. I.; Chimenos, J. M.; Lopez, J. M.; Espiell, F. Polym Degrad Stab 2007, 92, 1082.
2. Birnbaum, L. S.; Staskal, D. F. Environ Health Perspect 2004, 112, 9.
3. Szep, A.; Szabo, A.; Toth, N.; Anna, P.; Marosi, G. Polym Degrad Stab 2006, 91, 593.
4. Beyer, G. Fire Mater 2001, 25, 193.
5. Vostovich, J. E. US Pat.4459,380, 1984.
6. Zhang, X. G.; Guo, F.; Chen, J. F.; Wang, G. Q.; Liu, H. Polym Degrad Stab 2005, 87, 411.
7. Zhang, S.; Horrocks, A. R.; Hull, R.; Kandola, B. K. Polym Degrad Stab 2006, 91, 719.
8. Qin, H.; Su, Q.; Zhang, S.; Zhao, B.; Yang, M. Polymer 2003, 44, 7533.
9. Bourbigot, S.; Gilman, J. W.; Wilkie, C. A. Polym Degrad Stab 2004, 84, 483.
10. Gong, F.; Feng, M.; Zhao, C.; Zhang, S.; Yang, M. Polym Degrad Stab 2004, 84, 289.
11. Patiño, A. P.; Sánchez-Valdes, S.; Ramos-de Valle, L. F. J Polym Sci Part B: Polym Phys 2008, 46, 190.
12. Cross, M. S.; Cusack, P. A.; Hornsby, P. R. Polym Degrad Stab 2003, 79, 309.
13. Zanetti, M.; Camino, G.; Canavese, D.; Morgan, A. B.; Lamelas, F. J.; Wilkie, C. A. Chem mater 2002, 14, 189.
14. Morgan, A. B. Polym Adv Technol 2006, 17, 206.
15. Zhang, H.; Wang, Y.; Wu, Y.; Zhang, L.; Yang, J. J Appl Polym Sci 2005, 97, 844.
16. Schartel, B.; Knoll, U.; Hartwig, A.; Putz, D. Polym Adv Technol 2006, 17, 281.
17. Ray, S. S.; Okamoto, M. Prog Polym Sci 2003, 28, 153.
18. Roman-Lorza, S.; Rodriguez-Perez, M. A.; Saez, J. A. D. J Cell Plast 2010, 46, 259.
19. Jiao, C. M.; Chen, X. L.; Zhang, J. J Thermoplast Comp Mats 2010, 23, 501.
20. Riva, A.; Camino, G.; Pomperie, L.; Amigouet, P. Polym Degrad Stab 2003, 82, 341.
21. Anna, P.; Marosi, G.; Bourbigot, S.; Le Bras, M.; Delobel, R. Polym Degrad Stab 2002, 77, 243.
22. Faghihi, J.; Morshedian, J.; Ahmadi, S. Polym Polym Comp 2010, 18, 113.
23. Kaynak, C.; Gunduz, H. O.; Isitman, N. A. J Nanosci Nanotech 2010, 10, 7374.
24. Schall, N.; Engelhardt, T.; Simmler-Hubenthal, H.; Beyer, G. Ger. Pat. DE 199,21,472A1,2000.
25. Bartholmai, M.; Schartel, B. Polym Adv Technol 2004, 15, 355.

26. Yeh, J. T.; Yang, H. M.; Huang, S. S. Polym Degrad Stab 1995, 50, 229.
27. Basfar, A. A.; Mosnacek, J.; Shukri, T. M.; Bahattab, M. A.; Noireaux, P.; Courdreuse, A. J Appl Polym Sci 2008, 107, 642.
28. Valera, Z. M.; Ramírez-Vargas, E.; Medellín-Rodriguez, F. J Appl Polym Sci 2008, 108, 1986.
29. Vaia, R. A.; Giannelis, E. P. Macromolecules 1997, 30, 8000.
30. Lee, J.; Lim, Y.; Park, O. Polym Bull 2000, 45, 191.
31. Koo, C. M.; Kim, S. O.; Chung, I. J. Macromolecules 2003, 36, 2748.
32. Chen, L.; Wong, S. C.; Pisharath, S. J Appl Polym Sci 2003, 88, 3298.
33. Samyn, F.; Bourbigot, S.; Jama, C.; Bellayer, S.; Nazare, S.; Hull, R.; Fina, A.; Castrovinci, A.; Camino, G. Eur Polym J 2008, 44, 1631.
34. Haurie, L.; Fernandez, A. I.; Velasco, J. I.; Chimenos, J. M.; Tico-Grau, J. R.; Espiell, F. Macromol Symp 2005, 221, 165.
35. Chuang, T.; Wenjeng, G.; Cheng, K. C.; Chen, S. W.; Wang, H. T.; Yen, Y. J Mater Res 2004, 11, 169.
36. Gilman, J. W.; Jackson, C. L.; Morgan, A. B.; Harris, R. Chem Mater 2000, 12, 1866.
37. Ulutan, S.; Gilbert, M. J Mater Sci 2000, 35, 2115.
38. Nguyen, Q. T.; Baird, D. G. Polymer 2007, 48, 6923.
39. Samyn, F.; Bourbigot, S.; Jama, C.; Bellayer, S. Polym Degrad Stab 2008, 93, 201.
40. Isitman, N.; Kaynak, C. Polym Degrad Stab 2010, 95, 1759.